A host target of a bacterial cysteine protease virulence effector plays a key role in convergent evolution of plant innate immune system receptors

Maxim Prokchorchik[1,2], Sera Choi[1], Eui-Hwan Chung[3,4] (ID), Kyungho Won[5], Jeffery L. Dangl[3,4] (ID) and Kee Hoon Sohn[1,6] (ID)

[1]Department of Life Sciences, Pohang University of Science and Technology, Pohang 37673, Korea; [2]Bioprotection Research Centre, Institute of Agriculture and Environment, Massey University, Palmerston North 4474, New Zealand; [3]Department of Biology, University of North Carolina at Chapel Hill, Chapel Hill, NC 27599-3280, USA; [4]Howard Hughes Medical Institute, University of North Carolina at Chapel Hill, Chapel Hill, NC 27599-3280, USA; [5]National Institute of Horticultural and Herbal Science (NIHHS), Rural Development Administration (RDA), Naju 54875, Korea; [6]School of Interdisciplinary Bioscience and Bioengineering, Pohang University of Science and Technology, Pohang 37673, Korea

Summary

Author for correspondence:
Kee Hoon Sohn
Tel: +82 54 279 2357
Email: khsohn@postech.ac.kr

• Some virulence effectors secreted from pathogens target host proteins and induce biochemical modifications that are monitored by nucleotide-binding and leucine-rich repeat (NLR) immune receptors. Arabidopsis RIN4 protein (AtRIN4: RPM1-interacting protein 4) homologs are present in diverse plant species and targeted by several bacterial type III effector proteins including the cysteine protease AvrRpt2.
• RIN4 is 'guarded' by several independently evolved NLRs from various plant species, including Arabidopsis RPS2. Recently, it was shown that the MR5 NLR from a wild apple relative can recognize the AvrRpt2 effector from Erwinia amylovora, but the details of this recognition remained unclear.
• The present contribution reports the mechanism of AvrRpt2 recognition by independently evolved NLRs, MR5 from apple and RPS2, both of which require proteolytically processed RIN4 for activation. It shows that the C-terminal cleaved product of apple RIN4 (MdRIN4) but not AtRIN4 is necessary and sufficient for MR5 activation. Additionally, two polymorphic residues in AtRIN4 and MdRIN4 are identified that are crucial in the regulation of and physical association with NLRs.
• It is proposed that polymorphisms in RIN4 from distantly related plant species allow it to remain an effector target while maintaining compatibility with multiple NLRs.

Introduction

Many plant pathogens rely on effector proteins that are delivered into host cells to overcome innate immunity. However, plants have developed disease resistance (R) proteins which function to recognize effectors (Jones & Dangl, 2006; Dodds & Rathjen, 2010). The main class of R-proteins are intracellular nucleotide-binding (NB) and leucine-rich repeat (LRR) immune receptors (NLRs) with variable N-termini, primarily coiled-coil (CC) or toll/interleukin 1 receptor-like (TIR) domains. Effector-triggered immunity (ETI) is achieved when NLRs detect corresponding effector proteins either directly or indirectly.

Direct recognition of effectors often involves physical binding of the ligand (effector) to the corresponding NLR. Indirect recognition of an effector by an NLR protein occurs when an NLR detects the action of an effector on its host target (termed either a 'guardee' or a 'decoy'; Jones & Dangl, 2006; van der Hoorn & Kamoun, 2008). For example, resistance protein RESISTANT TO P. SYRINGAE 5 (RPS5) is an NLR that detects the cleavage

of Arabidopsis protein kinase AvrPphB SUSCEPTIBLE 1 (PBS1) by the *Pseudomonas syringae* pv *phaseolicola* effector protease AvrPphB (Swiderski & Innes, 2001; Shao *et al.*, 2003; Ade *et al.*, 2007). In some cases, absence or significant perturbation of the guardee or decoy can activate NLR-dependent immunity (Bonardi *et al.*, 2011; Rodriguez *et al.*, 2016).

The AvrRpt2 effector is a cysteine protease first identified in *P. syringae* pv *tomato* strain JL1065 (Whalen *et al.*, 1991). AvrRpt2 is delivered into the plant cell in a pre-active form and a plant prolyl-peptidyl isomerase (PPIase), ROC1, stimulates AvrRpt2 activity to cleave itself. This releases the active form of AvrRpt2, which is directed to the plant plasma membrane where it can cleave its plant targets (Nimchuk *et al.*, 2000; Coaker *et al.*, 2005; Coaker *et al.*, 2006). AvrRpt2 homologs are present in several bacterial pathogens and play important roles in their pathogenesis (Eschen-Lippold *et al.*, 2016). An AvrRpt2 homolog from *Erwinia amylovora*, the causal agent of bacterial fire blight in apple and pear, shares 62% protein sequence identity with the well-studied AvrRpt2 from

P. syringae. Pseudomonas syringae AvrRpt2 is known to suppress host defenses, including pattern-triggered immune responses, pathogenesis-related (PR) gene expression, typically induced by salicylic acid (SA) and auxin/indole acetic acid protein (Aux/IAA) pathway-dependent responses by promoting Aux/IAA turnover (Yamada, 1993; Chen *et al.*, 2004; Kim M. G. *et al.*, 2005; Cui *et al.*, 2013). AvrRpt2 also plays a critical role in *E. amylovora* pathogenesis because expression of this effector in apple plants is sufficient to cause disease symptoms (Zhao *et al.*, 2006; Schropfer *et al.*, 2018).

The RPM1-INTERACTING PROTEIN 4 (RIN4) guardee is an important plant immunity regulator and present in diverse plant species (Toruno *et al.*, 2018). AtRIN4 was shown to be a target of several sequence-unrelated bacterial effectors in Arabidopsis, including AvrB, AvrRpm1, AvrRpt2 and HopF2 (Mackey *et al.*, 2002; Mackey *et al.*, 2003; Wang *et al.*, 2010; Wilton *et al.*, 2010; Chung *et al.*, 2011). Effector-mediated post-translational modifications of RIN4 activate NLRs RESISTANCE TO *PSEUDOMONAS SYRINGAE* PV *MACULICOLA* 1 (RPM1) or RESISTANCE TO *PSEUDOMONAS SYRINGAE* 2 (RPS2) in Arabidopsis (Mackey *et al.*, 2002; Mackey *et al.*, 2003; Belkhadir *et al.*, 2004). AvrB induces phosphorylation of RIN4 (Chung *et al.*, 2011; Liu *et al.*, 2011; Chung *et al.*, 2014) and AvrRpm1 likely induces ribosylation of RIN4 (Cherkis *et al.*, 2012). Either of these post-translational modifications is sufficient to activate the CC-NLR (CNL) RPM1. RPM1 and RIN4 form a pre-activation complex in which all domains of RPM1 are required for activation upon RIN4 phosphorylation (El Kasmi *et al.*, 2017). This phosphorylation of RIN4 is executed by the RPM1-induced protein kinase (RIPK) and several other receptor-like cytoplasmic kinases (RLCKs), which act as a complex to phosphorylate RIN4 at three residues (T21, S160 and T166) (Liu *et al.*, 2011; Xu *et al.*, 2017). Phosphorylation of RIN4 at T166 is both necessary and sufficient to activate RPM1-mediated immunity in Arabidopsis (Chung *et al.*, 2011). Conversely, AtRIN4 is cleaved by *P. syringae* AvrRpt2, thus activating the guard CNL, RPS2 (Mackey *et al.*, 2002; Axtell & Staskawicz, 2003; Mackey *et al.*, 2003). Consistent with this, absence of AtRIN4 leads to lethal RPS2-mediated auto-immunity (Mackey *et al.*, 2002; Axtell & Staskawicz, 2003; Belkhadir *et al.*, 2004).

AtRIN4 homologs contain two highly conserved NOI (nitrate-induced) domains and a putative palmitoylation site (C203, C204, C205) at the C-terminus, allowing RIN4 tethering to the plasma membrane (Kim H. S. *et al.*, 2005; Takemoto & Jones, 2005; Afzal *et al.*, 2011). AvrRpm1, AvrB and AvrRpt2 also are localized to the plasma membrane via N-terminal myristoylation and, importantly, the plasma membrane localization of RIN4, RPM1 and AvrRpm1/AvrB are required for ETI (Nimchuk *et al.*, 2000; Jin *et al.*, 2003). Both AtRIN4 NOI domains carry RIN4 cleavage sites (RCS) with a consensus sequence [LVI]PxFGxW (where x represents any amino acid), which are proteolytically cleaved by AvrRpt2, resulting in three truncated products termed AvrRpt2-cleavage product (ACP): ACP1 (AA1-9), ACP2 (AA10-151) and ACP3 (AA152-211) (Chisholm *et al.*, 2005). These cleavage products were shown to negatively regulate PTI and promote

bacterial growth (Afzal *et al.*, 2011). The C-terminal half of AtRIN4 is necessary and sufficient for the suppression of RPS2 auto-activity, but none of the individual cleavage products alone can negatively regulate RPS2, supporting the model that cleavage of RIN4 specifically at RCS2 leads to RPS2 activation via loss of suppression by RIN4 (Day *et al.*, 2005; Kim H. S. *et al.*, 2005).

Apart from the aforementioned domains, amino acid sequences of AtRIN4 orthologs from different plant species are highly polymorphic and predicted to be intrinsically disordered (Kim H. S. *et al.*, 2005; Takemoto & Jones, 2005; Afzal *et al.*, 2011; Sun *et al.*, 2014). This intrinsic disorder is hypothesized to enable flexibility to interact with a number of signaling partners and thus might be important for the ability of RIN4 to act as a signaling hub (Rikkerink, 2018). However, mechanistic details of RIN4 diversification and the roles of AvrRpt2-processed RIN4 fragments in activation or suppression of NLR function is largely unknown.

Sequence and functional diversification of NLRs have been shown previously. In soybean two closely related CNLs, the RESISTANCE TO *PSEUDOMONAS SYRINGAE* PV *GLYCINEA*-B (RPG1-B) and RESISTANCE TO *PSEUDOMONAS SYRINGAE* PV *GLYCINEA*-R (RPG1-R) sharing 90% amino acid sequence identity with each other associate with four soybean RIN4 homologs (GmRIN4a-d) to detect either AvrB or AvrRpm1, respectively (Selote & Kachroo, 2010; Ashfield *et al.*, 2014; Kessens *et al.*, 2014). Note that this is by contrast to Arabidopsis, where the sequence unrelated CNL, RPM1, recognizes both effectors, suggesting convergent evolution of NLR function. In apple, a CNL gene *MR5* (*Malus × robusta5*) confers disease resistance to the fire blight pathogen *Erwinia amylovora* expressing AvrRpt2 (Vogt *et al.*, 2013; Broggini *et al.*, 2014). The mechanistic details of this resistance are obscure and comprise the basis of the present study. Apple contains two RIN4 homologs, MdRIN4-1 and MdRIN4-2, each sharing around 43% amino acid identity with Arabidopsis RIN4 (Vogt *et al.*, 2013). Intriguingly, MR5 and Arabidopsis RPS2 share only 22% protein sequence identity. This led the present authors to question whether there is an undiscovered property of RIN4 required for the activation of MR5.

The present contribution reports on a novel mode of AvrRpt2 effector recognition by MR5. It demonstrates that there is a unique requirement of the MdRIN4-1 for MR5 activation. A tight association is revealed between RIN4 homolog activity and the specific CNLs present in two distantly related plant species. Similar to Arabidopsis RPS2, the cleavage of MdRIN4-1 by *E. amylovora* AvrRpt2 is required for the activation of MR5. Interestingly, and clearly distinct from the AtRIN4, MdRIN4-1 does not appear to suppress NLR-dependent auto-activity. Instead, ACP3 released upon cleavage of MdRIN4-1 by AvrRpt2 is necessary and sufficient to activate MR5. Through comparative analysis of AtRIN4 and MdRIN4-1 variants, it is further demonstrated that RIN4 natural variants use distinct mechanisms to differentially regulate independently evolved NLRs.

Materials and Methods

Bacterial strains growth and transformation

Escherichia coli strain DH5α or *Agrobacterium tumefaciens* AGL1 was grown on Luria–Bertani (LB) liquid and solid agar medium containing appropriate antibiotics at 37°C or 28°C. *Pseudomonas syringae* pv *tomato* DC3000 and *P. fluorescens* Pf0-1 were grown in King's B medium at 28°C. All plasmids used in this study were transformed into *E. coli* or *A. tumefaciens* AGL1 using electroporation or into *Pseudomonas* by triparental mating.

Plant growth

Nicotiana benthamiana plants were grown in long-day conditions with 16 h : 8 h, light : dark at 24°C for 5 wk before use for *Agrobacterium*-mediated transient expression assays. *Arabidopsis thaliana* plants were grown in short-day conditions with 11 h : 13 h, light : dark at 22°C for 4–5 wk before use for *P. syringae* or *P. fluorescens* infiltration. For both *N. benthamiana* and *A. thaliana*, humidity was not controlled and was *c*. 60–70%.

Primer design and plasmid construction

Primers for PCR amplification (for details, see Supporting Information Table S1) of desired DNA fragments were designed to carry the *Bsa*I restriction sites with the overhangs required for Golden Gate (Engler *et al.*, 2008) assembly. PCR amplification was performed according to manufacturers' guidelines. Apple RPM1-INTERACTING PROTEIN 4 (RIN4) homologs and *MR5* genes were synthesized based on the sequence information obtained from NCBI for *Malus domestica* cultivar Golden Delicious and *Malus* × *robusta5*, respectively. All binary plasmids were constructed using the Golden Gate cloning method (Engler *et al.*, 2008) as described previously (Jayaraman *et al.*, 2017).

Site-directed mutagenesis

Site-directed mutagenesis was performed using the Quikchange Site-directed mutagenesis kit (Agilent, Santa Clara, CA, USA). Mutagenized plasmids were transformed into *E. coli* DH5α competent cells for selection and confirmation by Sanger sequencing.

Agroinfiltration and PCD assay

Agrobacterium tumefaciens AGL1 were grown on low-salt LB media containing appropriate antibiotics for 2 d at 28°C. Single colonies of freshly grown *A. tumefaciens* cells were isolated and used for inoculation of low-salt LB broth with antibiotics and grown overnight in a shaking incubator at 200 rpm. Overnight cultures were centrifuged at 2500 *g*, resuspended in infiltration buffer (10 mM MgCl$_2$, 10 mM MES), diluted to the desired concentration (OD$_{600}$ = 0.05 ~ 0.4) and then used for infiltrations into *N. benthamiana* leaves. Each infiltration was performed in at least four different leaf areas per experiment. Programmed cell death (PCD) was assayed at 2–3 d post-infection (dpi).

Ion leakage assay in *N. benthamiana*

The ion leakage measurement protocol described earlier was used with slight modifications (Oh *et al.*, 2010). Briefly, plants were agroinfiltrated with strains carrying constructs with genes of interest and 8-mm-diameter leaf discs were collected right after complete drying of the infiltrated area (0 dpi) and at 2 or 3 dpi when macroscopic PCD started to develop. Leaf discs for each time point were sampled independently, transferred to tissue culture plates containing sterile water and shaken for 2 h at 150 rpm before conductivity was measured using a Horiba compact (Kyoto, Japan) conductivity meter EC33. The mean conductivity of four to eight technical replicates was plotted on the graphs. One-way ANOVA test followed by Tukey–Kramer honest significant difference (HSD) analysis was performed to define the significant difference between measurements. Measurements with no significant difference are marked with the same letter. Different letters represent significant difference with *P*-value < 0.05.

Hypersensitive response and ion leakage assays in *A. thaliana*

Pseudomonas fluorescens Pf0-1 strains carrying pVSP61 empty vector (EV), pVSP61:AvrRpm1 (Ashfield *et al.*, 1995) or pVSP61:AvrPphB(Simonich & Innes, 1995) were hand-infiltrated into *A. thaliana* leaves before 10:00 h at OD$_{600}$ = 0.2 and resuspended in 10 mM MgCl$_2$ solution. The hypersensitive response (HR) development was photographed in 24 h post-infection (hpi). For ion leakage measurement, leaf discs were collected from infiltrated plants and washed for 30 min by gently shaking in distilled water. After that leaf discs were transferred to tissue culture plates filled with distilled water and conductivity was measured at 3, 6, 12 and 18 hpi using a Horiba compact conductivity meter EC33. Four technical replicates were plotted with error bars representing SEM.

Pseudomonassyringae pv *tomato* DC3000 growth curve assay in *A. thaliana*

P. syringae pv *tomato* DC3000 carrying pVSP61 EV, pVSP61: AvrRpm1 (Ashfield *et al.*, 1995) or pVSP61:AvrPphB (Simonich & Innes, 1995) were hand-infiltrated into *A. thaliana* leaves at OD$_{600}$ = 0.001 (5 × 10^5 CFU ml^{-1}) resuspended in 10 mM MgCl$_2$ solution. Leaf discs from infiltrated leaves were harvested at 2 hpi and 4 dpi then ground in 10 mM MgCl$_2$ solution. The number of bacteria recovered on plates from the serially diluted ground leaf disc solution was counted and results of four technical replicates were plotted with error bars representing SEM. Statistical significance was assessed by Student's *t*-test between selected sample and EV for that plant line: *, *P* < 0.05; **, *P* < 0.01.

Arabidopsis thaliana floral dip transformation

Agrobacterium tumefaciens AGL1 carrying pEpiGreen plasmids with RIN4 variants cDNA cloned downstream of 35S promoter and N-terminal Myc tag sequence were used to transform *A. thaliana* plants by the floral dip method (Clough & Bent, 1998). Transgenic plants were selected on soil by spraying the 10-d-old seedlings with Bayer BASTA solution (Leverkusen, Germany) and confirmed by semi-quantitative reverse transcription (RT)-PCR for transgene expression (for details see Methods S1). The T_2 seeds harvested from each confirmed T_1 parent line were used for experiments after three BASTA treatments.

Protein expression and extraction

Five-week-old *N. benthamiana* leaves were infiltrated with various *Agrobacterium* strains. *Agrobacterium*-infected leaf tissues were collected at 2 dpi and snap frozen in liquid nitrogen. Six frozen leaf discs for each protein sample were ground in a microtube, 200 µl of SDS protein loading buffer was added (250 mM Tris-HCl, 8% SDS, 40% Glycerol, 100 mM DTT, 0.1% Bromophenol blue), vortexed, boiled for 10 min at 96°C and loaded in SDS-PAGE gel for protein electrophoresis. If samples were subjected to co-immunoprecipitation (CoIP), *c.* 1 g of plant tissue was ground using a liquid nitrogen-chilled mortar and pestle, and transferred to an equal volume of protein extraction buffer (½ tablet of Sigma Complete™ mini protease inhibitor, NP-40 30 µl, DTT 75 µl, PVPP 0.15 g, GTEN Buffer to 15 ml), then thawed on ice before vortexing. Two milliliter of the sample was centrifuged at 2600 *g* at 4°C for 15 min and filtered through Merck MiraCloth (Kenilworth, NJ, USA). After 5× SDS protein loading buffer and samples were boiled at 96°C for 10min, they were vortexed then centrifuged at 12 000 *g* for 1 min.

SDS-PAGE and co-IP

SDS-polyacrylamide gel electrophoresis was performed to separate proteins by mass and subsequently blotted onto PVDF membranes. Proteins of interest were probed with horseradish peroxidase-conjugated antibodies specific for epitope tags (anti-HA (Santa-Cruz, Dallas, TX, USA), anti-FLAG (Sigma Aldrich) or anti-Myc (Cell Signaling, Danvers, MA, USA)). Epitope-tagged proteins were visualized using Super Signal West Pico and Femto reagents from Thermo Scientific. Chemiluminescence was detected by a GE ImageQuant (Boston, MA, USA) LAS 500 CCD imager. Approximate protein molecular weights can be found in Table S2. For Co-IP, total protein extracts were mixed with 15 µl of Sigma anti-FLAG beads and incubated on a rotary shaker at 4°C for 2 h. Subsequently, beads were gently centrifuged and the supernatant was discarded. Beads were incubated with IP buffer containing 3 × FLAG peptide for 45 min, to elute the proteins bound to beads. IP with anti-GFP (green fluorescent protein) was performed as described previously (El Kasmi *et al.*, 2017).

Results

MR5 recognizes AvrRpt2 via RIN4 cleavage

In a similar way to RESISTANT TO *P. SYRINGAE* 2 (RPS2) recognizing AvrRpt2 effector from *P. syringae*, MR5 was shown to recognize AvrRpt2 effector homolog from *Erwinia amylovora* (Vogt *et al.*, 2013). However, the coiled-coil (CC) and nucleotide-binding (NB) domains of MR5 do not share significant amino acid sequence identity with RPS2 (22%) and are more closely related to RESISTANCE TO *PSEUDOMONAS SYRINGAE* PV *GLYCINEA*-B (RPG1-B) (40%) and RESISTANCE TO *PSEUDOMONAS SYRINGAE* PV *GLYCINEA*-R (RPG1-R) (38%) (Fig. S1; Methods S2) suggesting that MR5 and RPS2 evolved independently. In order to test if the activation mechanism of MR5 is comparable to that of RPS2, we conducted *Agrobacterium*-mediated transient expression assays (hereafter, agroinfiltration) in *N. benthamiana*. All binary constructs used for agroinfiltration experiments in this study carried the Cauliflower mosaic virus 35S promoter except two experiments where native promoter was used for RPM1 expression as indicated in Figs 3(b) and 5(g). As expected, agroinfiltration of RPS2 alone triggered PCD which was suppressed by co-expression of *Arabidopsis thaliana* RIN4 (AtRIN4) (Day *et al.*, 2005). Moreover, co-expression of RPS2, AtRIN4 and the two wild-type (WT) PsAvrRpt2 (*P. syringae* AvrRpt2) or EaAvrRpt2 (*E. amylovora* AvrRpt2), but not cysteine protease activity-deficient mutants of each (PsAvrRpt2^{C122A} and EaAvrRpt2^{C88A}) induced PCD, also as shown previously (Fig. 1a; Day *et al.*, 2005). Next, it was tested whether, in a similar way to RPS2, the expression of MR5 alone induces PCD. By contrast to RPS2, agroinfiltration of MR5 alone or co-expression with either of the two *Malus domestica* RIN4 (MdRIN4) homologs (MdRIN4-1, RefSeq accession: NM_001293994.1 and MdRIN4-2, RefSeq accession: NP_001280834.1) did not induce PCD (Figs 1a, S2a). However, WT AvrRpt2 variants but not PsAvrRpt2^{C122A} or EaAvrRpt2^{C88A} induced strong PCD when co-expressed with MR5 and either of the MdRIN4 homologs or their orthologs from *Pyrus pyrifolia* or *P. ussuriensis* species (Figs 1a, S2a,b). Because protein sequences of apple RIN4 homologs, MdRIN4-1 and MdRIN4-2, are 91% identical and both could activate MR5 when co-expressed with AvrRpt2 (Figs 1a, S2a), MdRIN4-1 (hereafter, MdRIN4) was used in all subsequent experiments. In addition, it was tested if RIN4 homologs in *N. benthamiana* (NbRIN4) can play a role in regulating RPS2 or MR5 because this may cause confusion in interpretation of the results herein. When co-expressed in *N. benthamiana*, none of NbRIN4 homologs suppressed RPS2 auto-activity or activated MR5-dependent PCD in the presence of AvrRpt2. These results indicate that NbRIN4 homologs do not regulate RPS2 or MR5 (Fig. S3).

In order to test whether AvrRpt2-directed cleavage of RIN4 is required for MR5 activation, an immunoblot assay was performed using *N. benthamiana* leaf protein extracts transiently expressing epitope-tagged proteins. The WT AvrRpt2 variants but not PsAvrRpt2^{C122A} and EaAvrRpt2^{C88A} induced cleavage of AtRIN4 or MdRIN4 (Fig. 1b). This result indicated that cysteine

protease activity of AvrRpt2 is required for MR5 activation, self-processing and cleavage of both RIN4 natural variants from Arabidopsis and apple (Fig. 1b).

RIN4 variants possess different abilities to suppress and activate NLRs

Mutation of Asp to Val within the highly conserved MHD motif of the NB domain in NB and leucine-rich repeat (LRR) immune receptor (NLR) proteins causes auto-activation often results in PCD. By contrast, mutation of the P-loop motif critical for nucleotide binding and also located in the NB domain typically causes loss of NLR function (Bendahmane et al., 2002; Takken et al., 2006). To test if an MHV mutation of MR5 induces auto-activation that can be suppressed by RIN4 natural variants, site-directed mutagenesis was used to substitute D493 with V in the MR5 MHD motif. Agroinfiltration of $MR5^{D493V}$ induced P-loop motif-dependent PCD, because introduction of a second cis mutation in the P-loop motif, K206A, abolished $MR5^{D493V}$-induced PCD (Fig. 2a). In addition, co-expression of $MR5^{K206A}$, MdRIN4, and EaAvrRpt2 did not induce PCD, suggesting that, as expected, the P-loop motif is required for MR5 function. Immunoblot analysis confirmed that the loss of PCD by the K206A mutation is unlikely to be due to reduced protein abundance (Fig. 2b). However, MR5 protein was detected as two similar sized bands in total protein extracts. This could be due to an unknown post-translational modification because it is unlikely that alternative splicing would occur in the MR5 transcript, because it is not predicted to carry any introns.

Homologs of RIN4 are present in diverse plant species. In order to define the phylogenetic relationship of MdRIN4 and RIN4 natural variants whose function is known (e.g. AtRIN4 and GmRIN4), amino acid sequences of 119 representative RIN4 homologs were analyzed from 82 plant species (Fig. S4). The analysis herein showed that AtRIN4 is more closely related to MdRIN4 than GmRIN4 variants that were shown to be required for RPG1-B or RPG1-R-mediated effector recognition. Next, it was tested if MdRIN4 has different ability to regulate CNLs in comparison to AtRIN4. Interestingly, co-expression of MdRIN4 only weakly suppressed RPS2- or $MR5^{D493V}$-induced PCD, unlike AtRIN4 which strongly suppressed RPS2 (Fig. 2c). Immunoblot analysis showed comparable protein expression of RIN4 variants, demonstrating that the difference in suppression activity is not a result of differential protein abundance (Fig. 2d). The PCD phenotype was quantified by measuring ion leakage levels from leaves co-expressing RPS2 or $MR5^{D493V}$ with RIN4 variants or GFP, confirming the difference between AtRIN4 and MdRIN4 suppression activity on NLR auto-activity (Fig. 2e). Thus, MdRIN4 does not possess strong NLR-suppression function, whereas AtRIN4 suppresses RPS2. These data suggest divergent roles for these two RIN4 orthologs in the regulation of RPS2 and MR5 NLRs in the resting state.

In order to identify the RIN4 domains that confer functional variation in regard to NLR suppression and/or activation, two
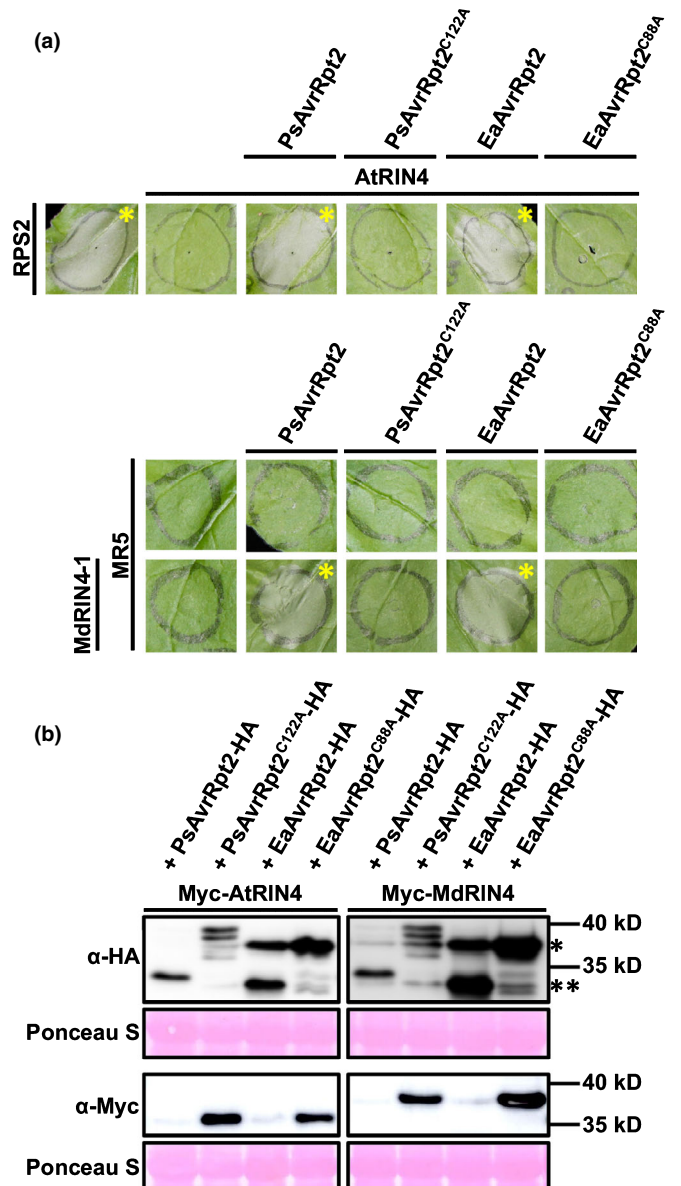

Fig. 1 AvrRpt2-directed cleavage of *Malus domestica* RPM1-INTERACTING PROTEIN 4 (MdRIN4) is recognized by *Malus × robusta5* (MR5). (a) MR5 and RPS2-mediated programmed cell death triggered by RIN4 cleavage by wild-type (WT) natural variants of AvrRpt2 in *Nicotiana benthamiana*. *Nicotiana benthamiana* was infiltrated with indicated mixture of *Agrobacterium* strains carrying *35S:MR5:FLAG* ($OD_{600} = 0.4$), *35S:RPS2:FLAG* ($OD_{600} = 0.1$), *35S:Myc:RIN4* ($OD_{600} = 0.4$) or *35S:AvrRpt2:HA* ($OD_{600} = 0.05$) variants. Programmed cell death (PCD) was photographed at 3 d post-infection (dpi). Yellow asterisks indicate agroinfiltrated leaf area showing PCD. The experiment was conducted more than three times with similar results. (b) *In planta* processing of AvrRpt2 and RIN4 variants. *Nicotiana benthamiana* leaves were infiltrated with Agrobacterium strains carrying *35S:Myc:RIN4* ($OD_{600} = 0.4$) and *35S:AvrRpt2:HA* ($OD_{600} = 0.2$) variants and leaf samples were taken for total protein extraction at 2 dpi. Total protein extracts were probed with anti-Myc or anti-HA antibody to visualize epitope-tagged proteins. Protein bands corresponding to the unprocessed and processed AvrRpt2 are marked with single and double asterisk respectively. Ponceau staining of the RuBisCO large subunit is provided to show equal protein loading.
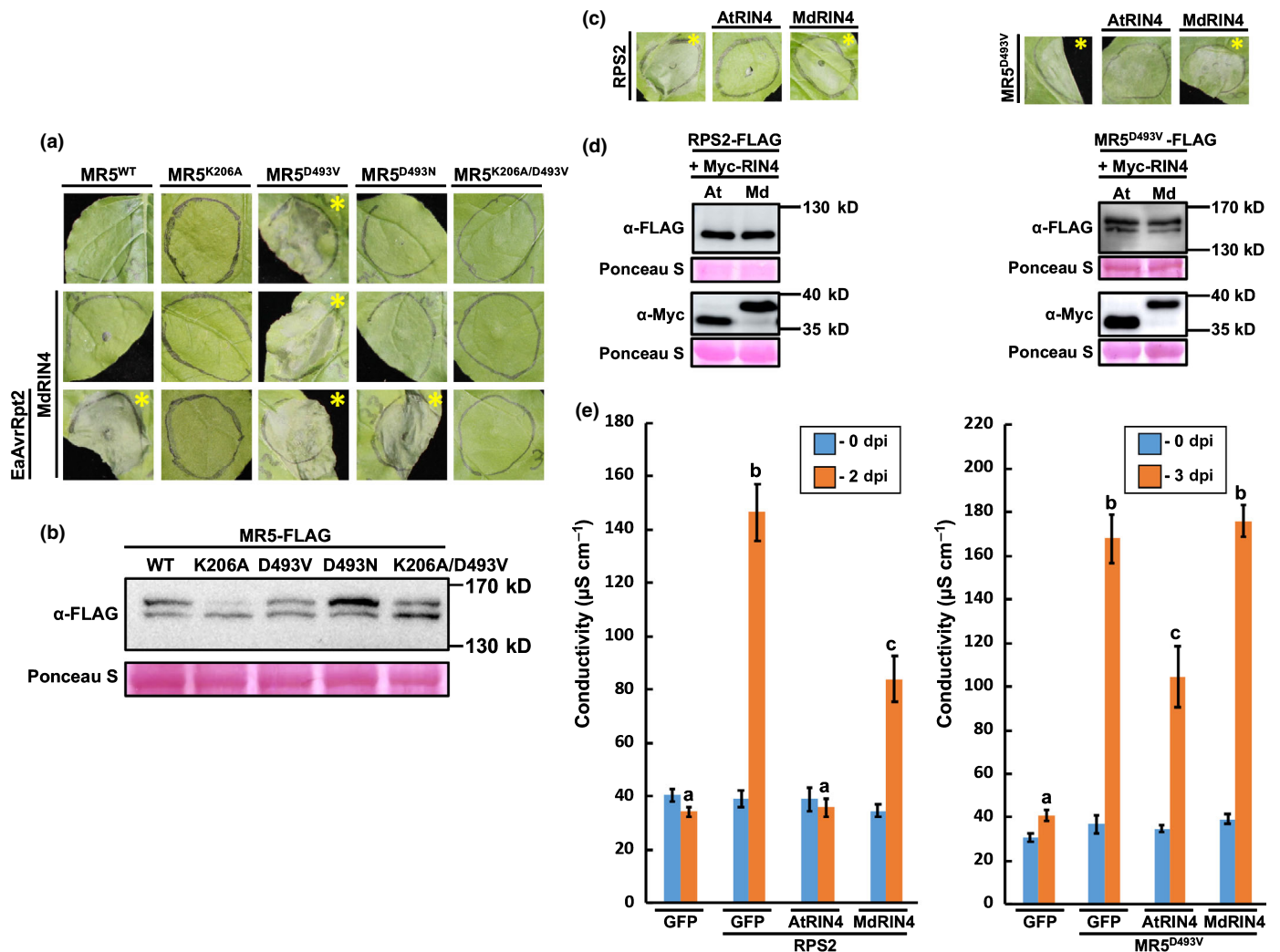
Fig. 2 RPM1-INTERACTING PROTEIN 4 (RIN4) natural variants have different abilities to suppress auto-active nucleotide-binding (NB) and leucine-rich repeat (LRR) immune receptors (NLRs). (a) An *Malus × robusta5* (MR5)^{K206A} mutation in the P-loop region abolishes MR5^{WT} and MR5^{D493V}-mediated programmed cell death (PCD). All MR5 variants and MdRIN4 were expressed via agroinfiltration with a mixture of strains carrying MR5 (OD$_{600}$ = 0.4), EaAvrRpt2 (OD$_{600}$ = 0.05) or MdRIN4 (OD600 = 0.4). Photographs were taken at 3 d post-infection (dpi). Yellow asterisks indicate agroinfiltrated leaf area showing PCD. The experiment was conducted more than three times with similar results. (b) Protein accumulation of MR5 variants *in planta*. Agroinfiltration and immunoblot analysis were performed as described in Fig. 1(b) except anti-FLAG antibody was used. (c) AtRIN4 but not MdRIN4 efficiently suppresses RPS2 or MR5^{D493V}-mediated PCD. The agroinfiltration assay was performed as described in Fig. 1(a) and photographs were taken at 2 dpi (for RPS2 suppression) or 3 dpi (for MR5^{D493V} suppression). Yellow asterisks indicate agroinfiltrated leaf area showing PCD. (d) AtRIN4 and MdRIN4 accumulate to a similar level *in planta*. Agroinfiltration and immunoblot analysis were performed as described in Fig. 1(b). RPS2-FLAG was immunoprecipitated with anti-FLAG agarose beads in order to avoid a nonspecific band. MR5^{D493V}-FLAG was detected from total protein extract without immunoprecipitation. Ponceau staining of the RuBisCO large subunit is provided to show equal protein loading. (e) MdRIN4 shows significantly reduced ability to suppress auto-activity induced by RPS2 or MR5^{D493V} in comparison to AtRIN4. The PCD symptoms were quantified via measurement of ion leakage levels from agroinfiltrated plant tissue. The agroinfiltration assay was performed as described in Fig. 1(a) and leaf samples were taken at the indicated time points for ion leakage measurement. Average values of eight electrolyte leakage measurements (*n* = 8) were plotted on the graph. Error bars represent SEM. Statistical significance was assessed by one-way ANOVA test followed by Tukey–Kramer honest significant difference analysis. Bars labeled with identical letters indicate that there is no significant statistical difference ($P > 0.05$). Final concentration (OD$_{600}$) of *Agrobacterium* strains were 0.1 for RPS2 and MR5^{D493V} and 0.4 for RIN4 variants and green fluorescent protein (GFP). The experiment was conducted three times with similar results.

RIN4 chimeras were generated with a domain swap at the well-conserved RCS2 site in the C-terminal nitrate-induced (NOI) domain (C-NOI) (Fig. 3a). Using RCS2 as a swap point was in agreement with previously published data showing the importance of the C-NOI region for both RPS2 suppression and RPM1 activation (Day *et al.*, 2005; Chung *et al.*, 2011). Additionally, these chimeras premitted shuffling of two major polymorphic regions of Arabidopsis RIN4 and apple natural variant (Fig. 3a). The A1-2M3 chimera carried N-terminal ACP1 and ACP2 from Arabidopsis fused with C-terminal ACP3 from apple. Conversely, the M1-2A3 chimera carried RIN4 ACP1 and ACP2 from apple and ACP3 from Arabidopsis. Interestingly, co-expression of A1-2M3 with MR5 and EaAvrRpt2 induced PCD. However, A1-2M3 did not support AvrRpm1-driven RPM1
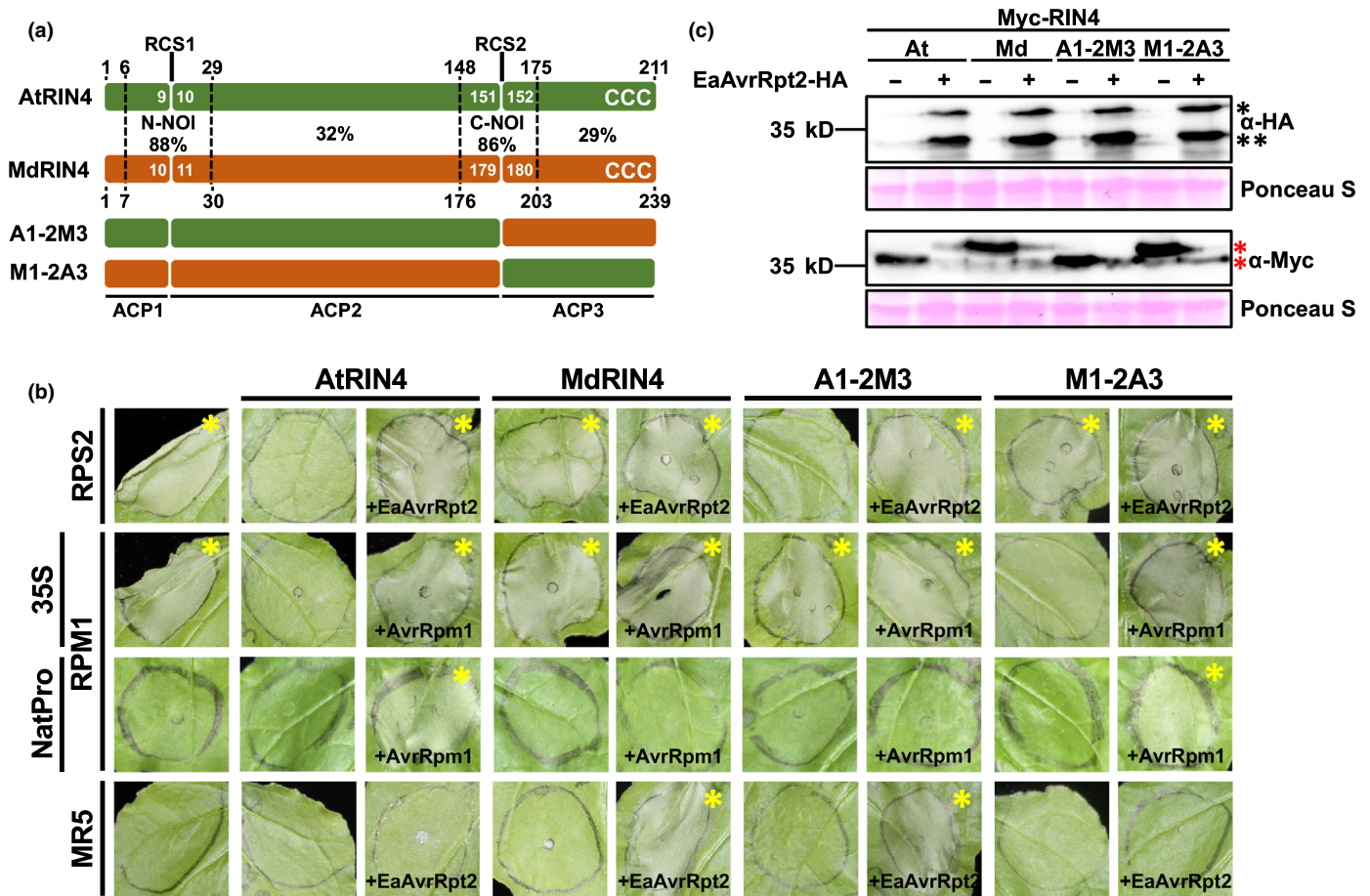
Fig. 3 C-terminal AvrRpt2-cleavage product (ACP3) of *Malus domestica* RPM1-INTERACTING PROTEIN 4 (RIN4) (MdRIN4) but not *Arabidopsis thaliana* AtRIN4 is critical for *Malus × robusta5* (MR5) activation (a) Schematic representation of wild-type (WT) and chimeric AtRIN4 and MdRIN4 variants. Percentage shows the level of protein sequence identity between AtRIN4 and MdRIN4 within the indicated regions. Numbers indicate the amino acid positions in the corresponding WT RIN4 proteins. CCC indicates the putative palmitoylation sequence. NOI, nitrate-induced domains (denoted by dashed lines); RCS, RIN4 cleavage site; ACP, AvrRpt2 Cleavage Product. (b) Distinct properties of RIN4 natural variants are required for suppression or activation of RPS2, RPM1 or MR5. RIN4 variants were expressed in *Nicotiana benthamiana* leaves using agroinfiltration. Agrobacterium densities (OD_{600}) used were: MR5 – 0.4, RPS2 – 0.1, RPM1 – 0.1, RIN4 variants – 0.4, EaAvrRpt2 – 0.05 and AvrRpm1 – 0.1. RPM1 was expressed from either the Cauliflower mosaic virus 35S promoter (35S) or native promoter (NatPro). Programmed cell death (PCD) development was photographed at 3 d post-infection (dpi). Yellow asterisks indicate agroinfiltrated leaf area showing PCD. The experiment was conducted three times with similar results. (c) RIN4 chimeric proteins accumulate to similar level and are processed by EaAvrRpt2 *in planta*. RIN4 chimeric proteins and AvrRpt2 variants were transiently expressed by using agroinfiltration with the concentration (OD_{600}) of 0.4 or 0.2 for RIN4 or EaAvrRpt2 variants, respectively, in *N. benthamiana* leaves. Tissue sampling and immunoblot analysis were performed as described in Fig. 1(b). Protein bands corresponding to the unprocessed and processed EaAvrRpt2 are marked with single and double asterisk respectively. Specific protein bands corresponding to the RIN4 chimeras are denoted with red asterisks. Ponceau staining of the RuBisCO large subunit is provided to show equal protein loading.

activation (RPM1 expressed from the native promoter (NatPro-RPM1)) (Fig. 3b). This suggests that the ACP3 domains of MdRIN4 and AtRIN4 are required for activation of MR5 and RPM1, respectively. Conversely, the M1-2A3 chimera induced PCD when co-expressed with NatPro-RPM1 and AvrRpm1, but not with MR5 and AvrRpt2, confirming that the AtRIN4 ACP3 region is required for RPM1 activation (Fig. 3b) (Chung *et al.*, 2011). In addition, A1-2M3 suppressed RPS2, but not 35S-RPM1 auto-activity. By contrast, M1-2A3 suppressed 35S-RPM1 but not RPS2 auto-activity (Fig. 3b). These results suggest that the sequence variation in the AtRIN4 ACP1-2 region is optimal for RPS2 suppression, but that the AtRIN4 ACP3 region is optimal for suppression of RPM1 auto-activation. Previously, it

was reported that the C-terminal half of AtRIN4 (106-211 AA), but not ACP3 is sufficient to suppress RPS2 auto-activity (Day *et al.*, 2005). Thus, it is plausible that the C-terminal region (106-151 AA) of AtRIN4 ACP2 plays an important role in suppressing RPS2 auto-activity. The latter result is consistent with previously reported data showing that the AtRIN4 C-terminal 70 amino acids, including the ACP3 fragment is sufficient to trigger AvrRpm1- or AvrB-mediated RPM1 activation in Arabidopsis (Fig. 3b; Chung *et al.*, 2011).

As reported previously, the absence of AtRIN4 in *rin4 rps2* Arabidopsis leads to weak RPM1-mediated immunity activation (Belkhadir *et al.*, 2004). Hence, RPM1 was expressed from its native promoter (NatPro-RPM1) in agroinfiltration experiments

to more closely approximate the native expression level of RPM1 (Belkhadir *et al.*, 2004). In this condition, agroinfiltration of RPM1 did not induce a detectable PCD at 2 dpi, whereas co-expression with AtRIN4 and AvrRpm1 led to rapid and robust PCD development (Fig. 3b). Interestingly, comparable PCD development was not observed when native promoter-driven RPM1 was co-expressed with MdRIN4 and AvrRpm1 (Fig. 3b). By contrast to the RPM1 system, co-expression of MR5 and MdRIN4, but not AtRIN4, induced PCD in the presence of EaAvrRpt2 suggesting an allele-specific requirement of MdRIN4 for MR5 activation (Fig. 3b). Therefore, AtRIN4 and MdRIN4 differ in requirements for both NLR suppression and activation. Both chimeric RIN4 proteins were well-expressed and efficiently processed by EaAvrRpt2, indicating that inability to suppress RPS2 or activate MR5 was not due to the lack of RIN4 protein stability or processing (Fig. 3c). Taken together, these results demonstrate that natural variations of RIN4 regions are differentially required to modulate sequence-unrelated NLRs from distantly related plant species.

MdRIN4 ACP3 is necessary and sufficient for activation of MR5

Mutation of Phe to Ala in the position 151 of AtRIN4 RCS2 causes loss of AvrRpt2-directed cleavage resulting in the loss of RPS2 activation (Chisholm *et al.*, 2005; Kim H. S. *et al.*, 2005). In order to investigate whether EaAvrRpt2-directed cleavage of MdRIN4 is required for MR5 activation, two mutations, F10A and F179A, that would abolish AvrRpt2-mediated MdRIN4 cleavage were introduced into RCS1 or RCS2 (Chisholm *et al.*, 2005). When each MdRIN4 variant (F10A, F179A or F10A/F179A) was co-expressed with EaAvrRpt2 and MR5, MdRIN4 F179A or F10A/F179A, by contrast to F10A, failed to activate MR5-dependent PCD (Figs 4a, S5). This result supports the hypothesis that cleavage at RCS2 by AvrRpt2 and ACP3 of MdRIN4 is important for MR5 activation. Immunoblot analysis confirmed that the mutations at the RCS abolished corresponding EaAvrRpt2-dependent cleavage of MdRIN4 (Fig. 4b).

The observation that expression of MR5 alone does not lead to PCD implied that the processed form of MdRIN4 ACP3 may be sufficient to activate MR5-dependent PCD independent of AvrRpt2. To test this, each of the truncated RIN4 variants corresponding to ACP1, ACP2, or ACP3 of AtRIN4 or MdRIN4 was co-expressed with MR5 in *N. benthamiana*. As expected (Fig. 3b), full-length AtRIN4 or MdRIN4 did not activate MR5-dependent PCD without AvrRpt2 (Fig. 4c). By contrast, MR5 co-expressed with ACP3 from MdRIN4, but not AtRIN4, induced strong PCD in the absence of AvrRpt2 (Fig. 4c). In addition, alanine mutations of conserved cysteine residues (C231, C232 and C233) of the C-terminally located putative palmitoylation site of MdRIN4 ACP3 (ACP3_AAA) caused loss of MR5-dependent PCD, indicating that plasma membrane localization of MdRIN4 ACP3 is both necessary and sufficient for MR5 activation (Fig. 4c) (Kim H. S. *et al.*, 2005). Taken together, MdRIN4 positively mediates MR5 activation in response to
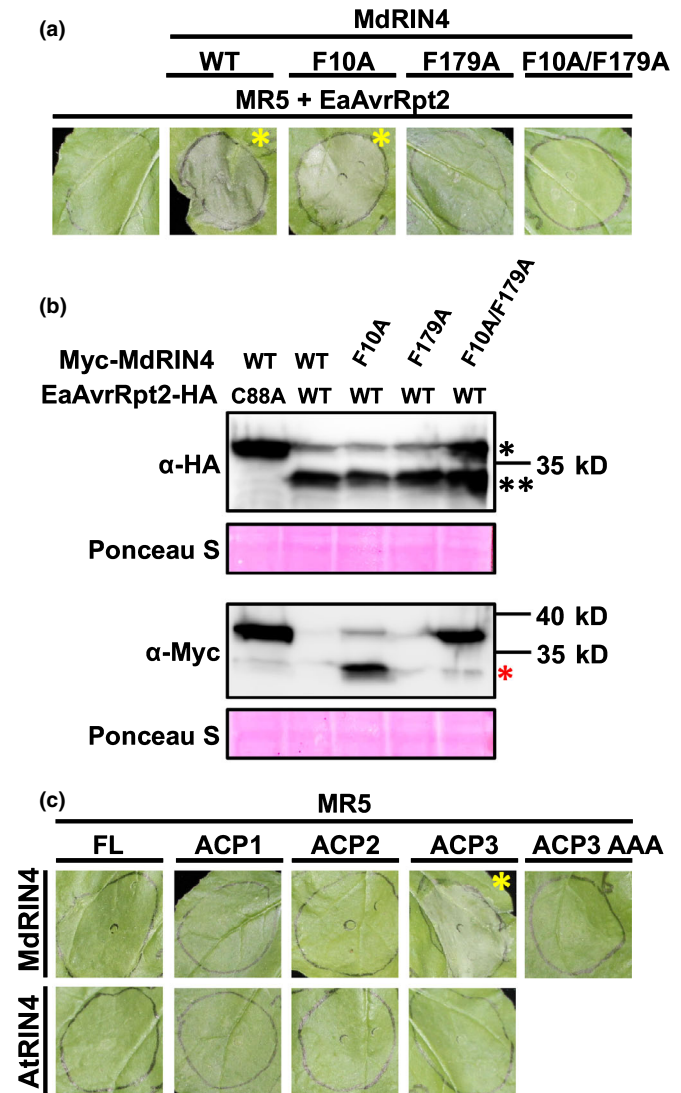

Fig. 4 *Malus domestica* RPM1-INTERACTING PROTEIN 4 (MdRIN4) ACP3 is sufficient to activate *Malus × robusta5* (MR5). (a) EaAvrRpt2-directed cleavage at RCS2 but not RCS1 is required for activation of MR5-dependent programmed cell death (PCD). The agroinfiltration assay was performed as described in Fig. 1(b) and photographs were taken 3 d post-infection (dpi). Yellow asterisks indicate agroinfiltrated leaf area showing PCD. The experiment was conducted three times with similar results. (b) Immunoblot analysis of MdRIN4 variants carrying RCS mutations. Mutations in RCS1 and RCS2 abolish the cleavage in corresponding sites. Agroinfiltration and immunoblot assays were performed as described in Fig. 1(b). Protein bands corresponding to the unprocessed and processed EaAvrRpt2 are marked with single and double asterisk respectively. Red asterisk shows the Myc-tagged N-terminal product derived from RIN4 cleavage at RCS2 exclusively. Ponceau staining of the RuBisCO large subunit is provided to show equal protein loading. (c) MdRIN4 ACP3 is sufficient to activate MR5-dependent PCD in absence of EaAvrRpt2. Full-length and truncated variants of AtRIN4 and MdRIN4 were transiently expressed by using agroinfiltration ($OD_{600} = 0.4$) with MR5 ($OD_{600} = 0.4$) in *Nicotiana benthamiana* leaves. Photographs were taken at 3 dpi. Yellow asterisks indicate agroinfiltrated leaf area showing PCD. The experiment was conducted three times with similar results.

AvrRpt2 via its C-terminal cleavage product, ACP3. This is mechanistically distinct from the negative regulation of RPS2 activity by AtRIN4.

Two amino acid residues in RIN4 ACP3 are critical for MR5 activation

Because the MdRIN4 ACP3 variant, but not the AtRIN4 ACP3 variant, can activate MR5, the polymorphisms between the AtRIN4 and MdRIN4 ACP3 segments were compared to identify critical residues required for MR5 activation (Fig. 5a). RIN4 ACP3 can be divided into two parts, based on sequence similarity between AtRIN4 and MdRIN4: a conserved N-terminal region containing part of the C-NOI domain and a variable C-terminal region. Accordingly, we generated chimeric RIN4 ACP3 variants as indicated in Fig. 5(a). Based on the sequence identity within ACP3, we further hypothesized that variation in the C-terminal polymorphic region in MdRIN4 ACP3 is critical for activation

of MR5. Surprisingly, the A-M-ACP3 chimera carrying the C-terminal polymorphic portion of MdRIN4 ACP3 did not activate MR5 (Fig. 5b). By contrast, the M-A-ACP3 chimera carrying the highly-conserved N-terminal portion of MdRIN4 ACP3 activated MR5 (Fig. 5b). Immunoblot analysis showed that AtRIN4 and MdRIN4 ACP3 accumulated to detectable levels and that the MR5 activation phenotype is not a product of allele-dependent ACP3 protein stability *in planta* (Fig. 5c). This is further supported by the fact that the A-M-ACP3 chimera could not activate MR5 even though its protein accumulation was higher than that of M-A-ACP3 (Fig. 5c).

In order to further dissect the mechanisms by which the MdRIN4, but not the AtRIN4, ACP3 activates MR5, we compared the highly conserved N-terminal sequences of AtRIN4
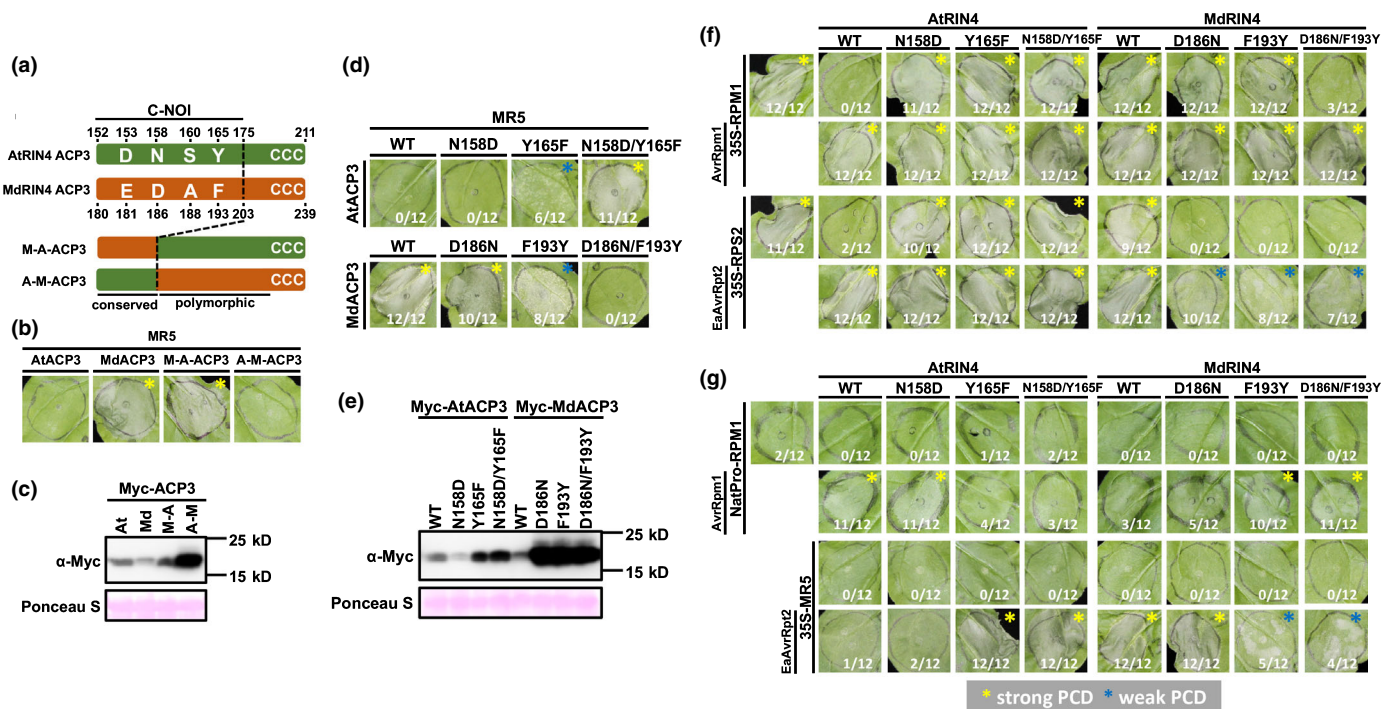

Fig. 5 Two amino acid residues in the conserved C-terminal nitrate-induced (NOI) domain of ACP3 are critical for nucleotide-binding (NB) and leucine-rich repeat (LRR) immune receptor (NLR) compatibility. (a) Schematic representation of wild-type (WT) and chimeric RPM1-INTERACTING PROTEIN 4 (RIN4) ACP3 variants. Four polymorphic amino acid residues in the C-NOI domain of ACP3 are indicated. Numbers indicate amino acid positions in AtRIN4 or MdRIN4. (b) The highly conserved C-NOI domain of MdRIN4 ACP3 is required for *Malus* × *robusta5* (MR5) activation. Indicated WT or chimeric ACP3 variants were co-expressed with MR5 in *Nicotiana benthamiana* via agroinfiltration (OD$_{600}$ = 0.4). Photographs were taken at 3 d post-infection (dpi). Yellow asterisks indicate agroinfiltrated leaf area showing programmed cell death (PCD). The experiment was conducted three times with similar results. (c) Immunoblot analysis of chimeric ACP3 variants. ACP3 variants were expressed via agroinfiltration (OD$_{600}$ = 0.4), samples were taken at 2 dpi and immunoblot analysis was performed as in Fig. 1(b). Ponceau staining of the RuBisCO large subunit is provided to show equal protein loading. (d) Reciprocal mutations at two polymorphic residues of AtRIN4 or MdRIN4 ACP3 alter MR5 activation. The agroinfiltration assay was carried out as described in Fig. 5(b). Yellow and blue asterisks indicate agroinfiltrated leaf area showing strong and weak PCD, respectively. Numbers on each panel represent the quantity of spots showing PCD out of total infiltrated spots. The experiment was conducted three times with similar results. (e) Immunoblot analysis of WT or mutant RIN4 ACP3 variants. Agroinfiltration and immunoblot analysis were performed as described in Fig. 5(c). Ponceau staining of the RuBisCO large subunit band is provided to show equal protein loading. (f) Mutations at two polymorphic residues alter RIN4-dependent suppression of 35S promoter-driven RPS2 and RPM1 auto-activity. The agroinfiltration assay was carried out as described in Fig. 5(b). Yellow and blue asterisks indicate agroinfiltrated leaf area showing strong and weak PCD, respectively. Numbers on each panel represent the quantity of spots showing PCD out of total infiltrated spots. The experiment was conducted three times with similar results. (g) Mutations at two polymorphic residues alter RIN4-dependent activation of RPM1 or MR5, when co-expressed with AvrRpm1 or EaAvrRpt2, respectively. The agroinfiltration assay was carried out as described in Fig. 5(f) except using native promoter-driven RPM1. Yellow and blue asterisks indicate agroinfiltrated leaf area showing strong and weak PCD, respectively. Numbers on each panel represent the quantity of spots showing PCD out of total infiltrated spots. The experiment was conducted three times with similar results. For panels describing native promoter driven RPM1 experiments, photographs of PCD were taken at 2 dpi due to significant RPM1 auto-activity at 3 dpi, whereas for the rest of panels photographs were taken at 3 dpi.

ACP3 (152–175 AA) and MdRIN4 ACP3 (180–203 AA) and identified four polymorphic amino acid residues (Fig. 5a). To test their requirement in MR5 activation, these four residues were individually mutated to the corresponding amino acids in the other RIN4 natural variant. It was found that introducing D153E or S160A mutations into A-M-ACP3 did not result in a gain of MR5 activation (Fig. S6). Likewise, the reciprocal mutations E181D or A188S in M-A-ACP3 did not abolish MR5 activation, suggesting that these residues do not play a significant role in MR5 activation. By contrast, introducing N158D and/or Y165F mutations into A-M-ACP3 resulted in activation of MR5, whereas reciprocal D186N and/or F193Y mutations in M-A-ACP3 led to a complete loss of MR5-dependent PCD (Fig. S6).

In order to test if identical mutations could alter WT ACP3 activity, each of the aforementioned mutations was introduced into MdRIN4 ACP3 and AtRIN4 ACP3 (Fig. 5d). The AtRIN4$^{N158D/Y165F}$ ACP3 variant strongly activated MR5. Conversely, MdRIN4$^{D186N/F193Y}$ ACP3 showed a complete loss of MR5 activation (Fig. 5d). Immunoblot analysis showed that the Y165F mutation appears to stabilize AtRIN4 ACP3 slightly, whereas the D186N or F193Y mutation in MdRIN4 ACP3 led to significantly higher protein accumulation (Fig. 5e). Therefore, it was concluded that enhanced ACP3 protein stability does not have direct correlation with stronger MR5 activation. In summary, the results herein indicate that the naturally occurring two amino acid variation in the C-NOI domain of AtRIN4 and MdRIN4 determines the specificity of the activation of RIN4-associated NLRs in Arabidopsis and apple.

The two polymorphic residues in RIN4 ACP3 are critical for suppression or activation of NLRs

Each of the reciprocal two amino acid swaps, or WT AtRIN4 or MdRIN4, were co-expressed with RPS2, RPM1, or MR5 in the presence or absence of corresponding effectors (Fig. 5f,g). Interestingly, the full-length AtRIN4$^{N158D/Y165F}$ variant, which activated MR5, did not suppress RPS2 or RPM1 auto-activity (Fig. 5f). By contrast, MdRIN4$^{D186N/F193Y}$ suppressed auto-activity of both RPM1 and RPS2 (Fig. 5f). Surprisingly, MdRIN4$^{D186N/F193Y}$, unable to activate MR5, showed significantly reduced ability to activate RPS2 as compared to WT AtRIN4 when co-expressed with EaAvrRpt2 (Figs 5f, S7). However, RPM1 activation in the presence of WT AtRIN4 or MdRIN4$^{D186N/F193Y}$ was indistinguishable when co-expressed with AvrRpm1 (Fig. 5f,g). These results indicate that RPS2 activation may require not only AvrRpt2-directed cleavage of RIN4 but also an unknown property of AtRIN4 that is absent in MdRIN4. In agreement with the authors' previous results (Fig. 5d), full-length AtRIN4$^{N158D/Y165F}$ activated MR5 when co-expressed with EaAvrRpt2, whereas it lost the ability to induce PCD in the presence of NatPro-RPM1 and AvrRpm1 (Fig. 5g). Conversely, MdRIN4$^{D186N/F193Y}$ had severely reduced ability to activate MR5 in the presence of EaAvrRpt2. Protein immunoblot analysis showed that all full-length RIN4 mutant variants accumulated to higher levels *in planta* in comparison to WT and were eliminated in the presence of EaAvrRpt2 (Fig. S8). Furthermore

the additional mutation of C-terminal membrane tethering sequence of RIN4 variants abolished their ability to suppress RPS2 auto-activity, as well as to activate MR5 in presence of AvrRpt2 indicating that the aforementioned mutations in NOI-domain did not significantly alter subcellular localization of RIN4 (Fig. S9a,c). In addition, protein accumulation levels of these RIN4 variants did not correlate with their ability to suppress RPS2 or activate MR5 (Fig. S9b,d) suggesting that changes in RIN4 protein abundance did not directly affect RIN4 function. Taken together, these data suggest that two polymorphic amino acid residues identified in RIN4 ACP3 play a critical role in suppressing or activating NLR function.

In order to further dissect the role of RIN4 ACP3 in suppression of RPS2 or RPM1 auto-activity, we co-expressed ACP3 variants with either RPS2 or RPM1 in *N. benthamiana*. Wild-type or AtRIN4$^{N158D/Y165F}$ ACP3 were unable to suppress either RPS2 or RPM1 auto-activity (Fig. S10a). However, MdRIN4 ACP3 showed partial suppression of RPS2 but not RPM1 auto-activity (Fig. S10a). Strikingly, the MdRIN4$^{D186N/F193Y}$ ACP3 completely suppressed PCD triggered by RPS2 or RPM1 (Fig. S10a). The PCD phenotypes observed were quantified by measuring ion leakage levels from plant tissues expressing combinations of RIN4 ACP3 variants and auto-active NLRs and were in agreement with macroscopic symptoms (Fig. S10b). Thus, it is plausible that MdRIN4 ACP3 may have a property that is absent in AtRIN4 ACP3 in suppression of NLR auto-activity. Because ACP3, but not full-length MdRIN4, partially suppressed RPS2 auto-activity, it is reasonable to hypothesize that MdRIN4 ACP1 and 2 may inhibit ACP3 function. However, the possibility cannot be rulef out that the enhanced suppression activity of MdRIN4$^{D186N/F193Y}$ ACP3 as compared to WT AtRIN4 could be due to a difference in protein stability (Fig. 5e).

Mutation in the two polymorphic RIN4 ACP3 residues is sufficient to alter association with NLRs

It was hypothesized that the critical residues in the N-terminal of ACP3 play a critical role in both effector-induced modification of RIN4 and RIN4-NLR physical association. It was shown that these residues do not affect AvrRpt2-directed RIN4 processing because both AtRIN4 and MdRIN4 are efficiently cleaved when co-expressed with AvrRpt2 (Fig. 3c). Co-immunoprecipitation was first used to test the role of these residues in RIN4–RPM1, RIN4-AvrRpm1 or RIN4–RIPK association following agroinfiltration in *N. benthamiana*. It was observed that the association of RPM1 with AtRIN4$^{N158D/Y165F}$ was lost, whereas MdRIN4$^{D186N/F193Y}$ association with RPM1 was enhanced (Fig. 6a). Previously, it was demonstrated that RIN4 phosphorylation is induced by AvrRpm1 via the Arabidopsis kinase RIPK (Chung *et al.*, 2011; Liu *et al.*, 2011). Neither of the RIN4 reciprocal swap mutants were altered in their ability to associate with RIPK (Fig. 6b). Interestingly, MdRIN4$^{D186N/F193Y}$ showed enhanced association with AvrRpm1 whereas AtRIN4$^{N158D/Y165F}$ had no effect (Fig. 6c). Nevertheless, the possibility cannot be ruled out that this enhanced association is due to the greater abundance of MdRIN4$^{D186N/F193Y}$ than MdRIN4 WT protein.
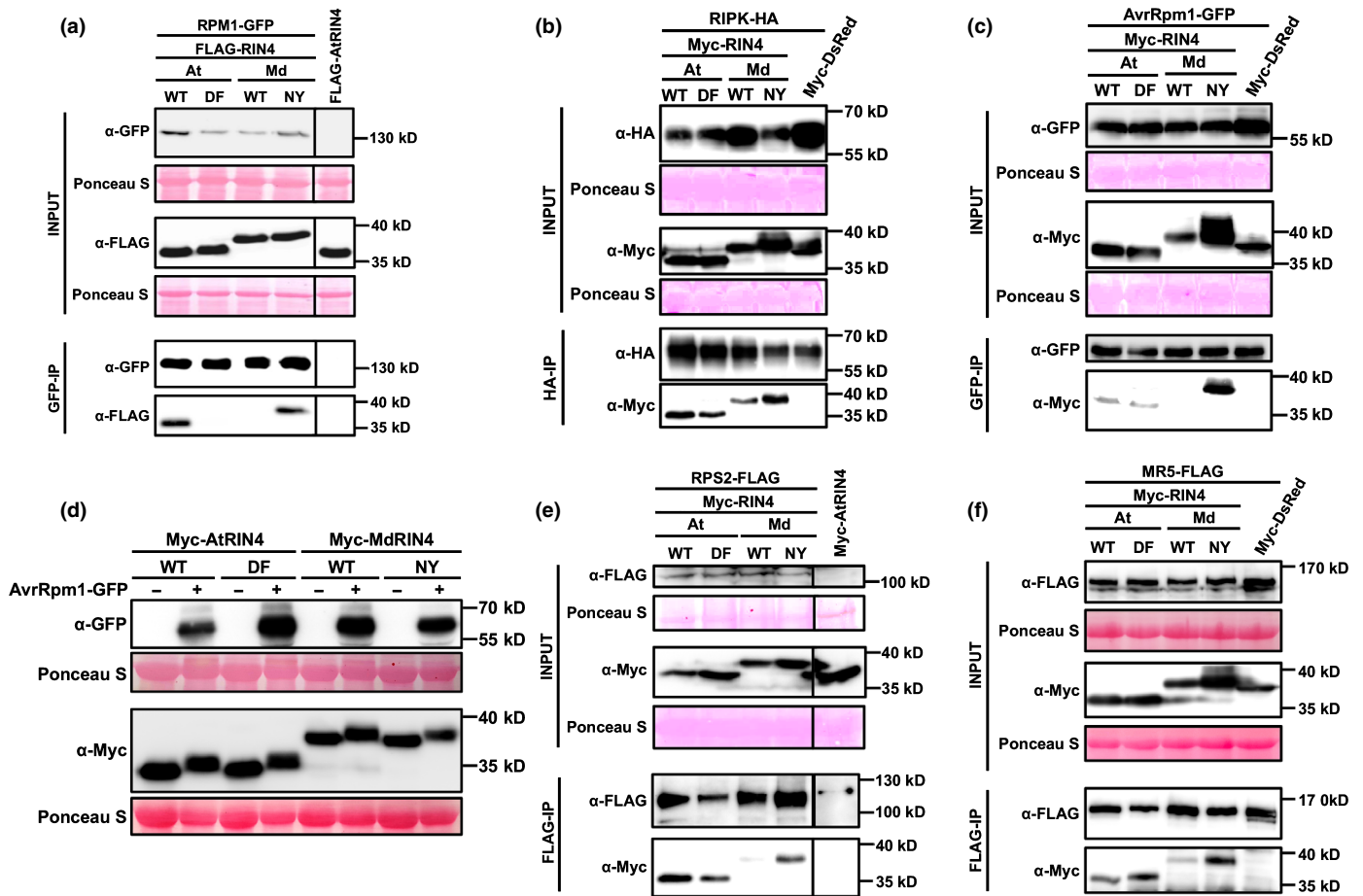
Fig. 6 Mutation in two polymorphic RPM1-INTERACTING PROTEIN 4 (RIN4) ACP3 residues is sufficient to alter association with nucleotide-binding (NB) and leucine-rich repeat (LRR) immune receptors (NLRs). (a) Mutations in two polymorphic residues cause altered RIN4-RPM1 association. RPM1-GFP (green fluorescent protein) expressed from the native promoter, AtRIN4 wild-type (WT), AtRIN4$^{N158D/Y165F}$ (DF), MdRIN4 WT and MdRIN4$^{D186N/F193Y}$ (NY) were infiltrated at OD_{600} of 0.2 for RPM1 and 0.4 for RIN4 variants. Immunoprecipitation with anti-GFP was performed, followed by Immunoblots with anti-GFP for RPM1 or anti-FLAG for RIN4 variants, respectively. Similar results were observed in two independent experiments. (b) Mutations in two polymorphic residues do not affect interaction of RIN4 variants with RIPK. Agrobacterium strains carrying RIN4 variants or RIPK were co-infiltrated at OD_{600} of 0.4. (c) MdRIN4$^{D186N/F193Y}$ shows increased interaction with AvrRpm1. Agroinfiltration was performed as described in (b) and OD_{600} for all *Agrobacterium* strains used was 0.4. (d) Mutations in the key polymorphic residues of RIN4 do not affect AvrRpm1-induced post-translational modification. Post-translational modification of RIN4 is inferred from the band-shift (Mackey *et al.*, 2002). Epitope-tagged proteins were transiently expressed in *Nicotiana benthamiana* leaves via agroinfiltration and leaves were sampled at 2 d post-infection (dpi). Total protein extracts were probed with anti-GFP and anti-Myc antibodies to visualize the proteins. Ponceau staining of the RuBisCO large subunit is provided to show equal protein loading of input samples. (e,f) MdRIN4$^{D186N/F193Y}$ shows significantly enhanced interaction with (e) RPS2 and (f) MR5 in comparison to MdRIN4. For all data shown in Fig. 6 epitope-tagged proteins were transiently expressed in *N. benthamiana* leaves via agroinfiltration and leaves were sampled at 2 dpi for total protein extraction. Total protein extracts were incubated with GFP-beads (a,c), HA-beads (b) or FLAG-beads (e,f) and immunoprecipitated proteins were probed with the indicated antibodies. Ponceau staining of the RuBisCO large subunit is provided to show equal protein loading of input samples.

Tests revealed that the enhanced association of MdRIN4$^{D186N/F193Y}$ and AvrRpm1 was not correlated with enhanced phosphorylation of MdRIN4, because all the RIN4 variants tested showed the protein band shift a characteristic for phosphorylated RIN4 (Fig. 6d). This experiment was extended to associations between MdRIN4$^{D186N/F193Y}$ and RPS2 or MR5 and greatly enhanced association was observed with either RPS2 or MR5 (Fig. 6e,f). However, AtRIN4$^{N158D/Y165F}$ association with RPS2 or MR5 was unaltered (Fig. 6e,f). Taken together, these results demonstrate that variation in the two critical polymorphic N-terminal ACP3 residues of RIN4 are sufficient to alter physical association of RIN4 with RPM1, RPS2 and MR5.

N158 and Y165 of AtRIN4 are required for activation of RPM1 in transgenic Arabidopsis lines

The AtRIN4 N158 and Y165 residues are required for activation of NatPro-RPM1 when transiently expressed in *N. benthamiana* (Fig. 3b). In order to confirm that these amino acids also are required for activating RPM1 in Arabidopsis, stable Arabidopsis transgenic lines were generated that constitutively expressed AtRIN4, AtRIN4$^{N158D/Y165F}$, MdRIN4 or MdRIN4$^{D186N/F193Y}$ in a *rin4 rps2* double homozygous mutant background. The mRNA expression of RIN4 variants in these transgenic plants (T_2 generation) was tested by semi-quantitative RT-PCR and

showed similar levels of expression (Fig. S11). It was not possible to generate transgenic Arabidopsis plants expressing RIN4 variants in the *rin4* homozygous mutant to test suppression of RPS2 auto-activity because *rin4* homozygous mutant is lethal (Mackey *et al.*, 2002; Axtell & Staskawicz, 2003). The leaves of transgenic plants were infiltrated with *P. fluorescens* Pf0-1 carrying a type III secretion system (hereafter, Pf0-1 (T3S)) (Thomas *et al.*, 2009) carrying EV, *avrRpm1* or *avrPphB* effector. Similar to the *N. benthamiana* transient expression results (Fig. 5g), only the lines expressing WT AtRIN4 or MdRIN4$^{D186N/F193Y}$ induced a HR and significant elevation in ion leakage level in response to

Pf0-1(T3S)-delivered AvrRpm1 (Fig. 7a,b). To test if HR development correlated with enhanced bacterial disease resistance, the transgenic lines were infected with virulent *P. syringae* pv *tomato* (*Pto*) DC3000 carrying EV, *avrRpm1* or *avrPphB* effector proteins. As expected, *Pto* DC3000 carrying EV or *avrPphB* displayed full susceptibility or resistance in all Arabidopsis genotypes tested, respectively. The growth of *Pto* DC3000 (*avrRpm1*) was restricted in WT Col-0, WT AtRIN4 and MdRIN4$^{D186N/F193Y}$ transgenic plants, but not in either *rin4 rps2* controls, AtRIN4$^{N158D/Y165F}$ or MdRIN4 transgenic plants. Consistent with the HR and ion leakage results herein (Fig. 7a,

Fig. 7 D186N and F193Y mutations are sufficient for *Malus domestica* RPM1-INTERACTING PROTEIN 4 (MdRIN4) activity in AvrRpm1-triggered immunity in transgenic Arabidopsis lines (a) Hypersensitive response and (b) ion-leakage triggered by bacterially-delivered AvrRpm1 or AvrPphB in transgenic Arabidopsis lines expressing RIN4 variants. Arabidopsis leaves were infiltrated with *Pseudomonas fluorescens* Pf0-1 (T3S) strains carrying empty vector (EV), *avrRpm1* or *avrPphB* ($OD_{600} = 0.2$). Leaves were photographed at 24 h post-infection (hpi). Yellow asterisks indicate agroinfiltrated leaf area showing. Electrolyte leakage from leaf tissue was measured with four technical replicates ($n = 4$) and error bars represent SEM. Statistical significance was assessed by Student's *t*-test between selected sample and EV at 18 hpi timepoint; ns, $P > 0.05$; *, $P < 0.05$; **, $P < 0.01$. The experiment was conducted three times with similar results. (c) *Pto* DC3000 growth restriction in transgenic Arabidopsis lines expressing RIN4 variants indicated in (a). Arabidopsis leaves were infiltrated (5×10^5 CFU ml^{-1}) with *Pto* DC3000 carrying EV, *avrRpm1* or *avrPphB* and bacterial growth was determined at 4 d post-infection (dpi). Error bars represent SEM. from four technical replicates. Statistical significance was assessed by Student's *t*-test between selected sample and EV; *, $P < 0.05$; **, $P < 0.01$. The experiment was conducted three times with similar results.

b), *Pto* DC3000 (*avrRpm1*) activated disease resistance that was dependent on AtRIN4 N158 and Y165 residues (Fig. 7c). These data further demonstrate the requirement of these amino acids in regulating RPM1 function.

Discussion

Multiple bacterial effectors target important immune regulators such as RPM1-INTERACTING PROTEIN 4 (RIN4). Effector-dependent post-translational modifications are recognized by corresponding nucleotide-binding (NB) and leucine-rich repeat (LRR) immune receptors (NLRs) in Arabidopsis (Mackey *et al.*, 2002; Axtell & Staskawicz, 2003; Mackey *et al.*, 2003; Wilton *et al.*, 2010; Chung *et al.*, 2011; Lee *et al.*, 2015). Convergently evolved NLRs also sense effector-induced RIN4 modification in other plant species (Ashfield *et al.*, 1995; Luo *et al.*, 2009; Selote & Kachroo, 2010; Kessens *et al.*, 2014). The present study shows that distinct mechanisms are required for sensing the AvrRpt2-dependent proteolytic cleavage of RIN4 by convergently evolved NLRs, RESISTANCE TO *PSEUDOMONAS SYRINGAE* 2 (RPS2) from Arabidopsis and *Malus × robusta5* (MR5) from apple. Significantly, the property of RIN4 required for determining activation of RPS2 or MR5 also is critical for RPM1. Thus, the specific polymorphic amino acids defined herein, AtRIN4 N158 and Y165 and MdRIN4 D186 and F193 can be critical targets of convergent NLR evolution. In addition to the significance of the present study in better understanding NLR evolution, the results herein provide essential information regarding fire blight resistance breeding. For instance, it would be important and necessary to identify the sequence variation at D186 and F193 of RIN4 when developing new apple varieties carrying MR5 for fire blight resistance.

The mechanism by which another effector protease, AvrPphB, activates the Arabidopsis coiled-coil (CC) NLR (CNL) RPS5 has been studied in detail. Cleavage of a receptor-like cytoplasmic kinase AvrPphB SUSCEPTIBLE 1 (PBS1) by AvrPphB, activates RPS5-dependent immune signaling in Arabidopsis (Swiderski & Innes, 2001; Shao *et al.*, 2003; Ade *et al.*, 2007). Neither fragment of PBS1 is sufficient to activate RPS5, although co-expression of both fragments is required (DeYoung *et al.*, 2012). Recently, it was shown that a barley NLR, PBR1 (AVRPPHB RESISTANCE 1), recognizes AvrPphB-directed cleavage of PBS1 (Carter *et al.*, 2018). However, in comparison with RPS5, the mechanistic basis of PBR1 recognition of processed PBS1 is unknown. Interestingly, a PBS1 ortholog identified from wheat (TaPBS1) is unable to activate RPS5 in the presence of AvrPphB (Sun *et al.*, 2017). Sun and colleagues further identified that two amino acid polymorphisms at a short SEMPH/STRPH motif in PBS1 confers variation in RPS5 activation (Sun *et al.*, 2017). By comparison to the data herein, it is hypothesized that the processed PBS1 C-terminal region might be sufficient to activate PBR1. It would be fascinating to compare RIN4 and PBS1 recognition systems in various plant species to better understand the mechanistic basis of convergent evolution of the plant immune system in the future.

In lettuce, RIN4 functions as a hybrid necrosis factor in the F_1 progeny derived from *Lactuca sativa* and *L. saligna* (Jeuken *et al.*, 2009). It is plausible that the *L. saligna* variant of RIN4 functions in a similar way to MdRIN4, lacking the ability to suppress an unknown NLR in *L. sativa* whose activity it negatively regulates, like AtRIN4 and RPS2. It is plausible that this NLR is not present or nonfunctional in *L. saligna*. In support of this hypothesis, three polymorphic residues located in the C-terminal half of *L. saligna* RIN4 were able to explain this lack of suppression, similar to the residue specificity observed for MdRIN4/AtRIN4. Moreover, in soybean, there are four RIN4 homologs guarded by RESISTANCE TO *PSEUDOMONAS SYRINGAE* PV *GLYCINEA*-B (RPG1-B) and RESISTANCE TO *PSEUDOMONAS SYRINGAE* PV *GLYCINEA*-R (RPG1-R) NLR proteins which confer recognition of AvrB and AvrRpm1, respectively (Ashfield *et al.*, 2014; Kessens *et al.*, 2014). Unlike detection of these two effectors by the same NLR in Arabidopsis (RPM1), soybean alleles recognize either AvrB (RPG1-B mediated) or AvrRpm1 (RPG1-R mediated) (Selote & Kachroo, 2010; Kessens *et al.*, 2014). By contrast to MdRIN4, RIN4 homologs from soybean form two relatively distant groups one including GmRIN4a and b, and the other GmRIN4c and d (Fig. S4). It would be interesting to test whether distinct mechanisms are required for soybean RIN4 homologs to activate RPG1R and RPG1-B.

Based on the discovery herein that a pair of simple sequence polymorphisms in the RIN4 ACP3 segment can switch between suppression and activation of NLRs, it is proposed that 'guardee evolution' may occur depending on the NLR landscape within distinct plant species. In this extension of the zigzag model (Jones & Dangl, 2006), where NLR genes can be under diversifying selection to detect pathogen effectors, it is hypothesized herein that, in some cases, guardee/decoy proteins also can be under selection pressure, where sequence changes in guardees/decoys enable activation or de-repression of independently evolved NLRs in different plant species. This is in line with the presence of intrinsically disordered regions in RIN4 which might be required for its ability to interact with a variety of NLRs and other immunity signaling components (Sun *et al.*, 2014). It is proposed that, by contrast to AtRIN4, MdRIN4 has a reduced ability to suppress NLR-triggered auto-activity due to the absence of a co-evolutionary history with auto-active NLRs like RPS2.

The minimal requirement of RIN4 to switch NLR compatibility identified in the present study implies that despite its important function RIN4 may be an adaptive protein. This indicates that, depending on the available NLRs within the genome of a given plant species, RIN4 may function as either a suppressor or activator of NLRs while maintaining its function in plant immunity regulation and ability to be biochemically modified by effectors for recognition. The discoveries herein suggest that the guardee or decoy can evolve alongside the diversifying NLR(s) and thus play a role in the co-evolutionary arms race between plants and pathogens in nature. Further investigation of RIN4 natural variants in terms of activation or suppression of NLRs may reveal more detailed mechanisms of RIN4 evolution and potentiate their use in developing disease resistant crop varieties.

Author contributions

MP and KHS designed the experiments; KW provided the material for pear RIN4 cloning; MP, SC and E-HC conducted the experiments; MP, E-HC and KHS prepared the figures; and MP, E-HC, JLD and KHS wrote the manuscript.

ORCID

Eui-Hwan Chung ⬭ https://orcid.org/0000-0002-5048-8142
Jeffery L. Dangl ⬭ https://orcid.org/0000-0003-3199-8654
Kee Hoon Sohn ⬭ https://orcid.org/0000-0002-9021-8649

References

Ade J, DeYoung BJ, Golstein C, Innes RW. 2007. Indirect activation of a plant nucleotide binding site-leucine-rich repeat protein by a bacterial protease. *Proceedings of the National Academy of Sciences, USA* 104: 2531–2536.

Afzal AJ, da Cunha L, Mackey D. 2011. Separable fragments and membrane tethering of *Arabidopsis* RIN4 regulate its suppression of PAMP-triggered immunity. *Plant Cell* 23: 3798–3811.

Ashfield T, Keen NT, Buzzell RI, Innes RW. 1995. Soybean resistance genes specific for different *Pseudomonas syringae* avirulence genes are allelic, or closely linked, at the *RPG1* locus. *Genetics* 141: 1597–1604.

Ashfield T, Redditt T, Russell A, Kessens R, Rodibaugh N, Galloway L, Kang Q, Podicheti R, Innes RW. 2014. Evolutionary relationship of disease resistance genes in soybean and *Arabidopsis* specific for the *Pseudomonas syringae* effectors AvrB and AvrRpm1. *Plant Physiology* 166: 235–251.

Axtell MJ, Staskawicz BJ. 2003. Initiation of RPS2-specified disease resistance in *Arabidopsis* is coupled to the AvrRpt2-directed elimination of RIN4. *Cell* 112: 369–377.

Belkhadir Y, Nimchuk Z, Hubert DA, Mackey D, Dangl JL. 2004. *Arabidopsis* RIN4 negatively regulates disease resistance mediated by RPS2 and RPM1 downstream or independent of the NDR1 signal modulator and is not required for the virulence functions of bacterial type III effectors AvrRpt2 or AvrRpm1. *Plant Cell* 16: 2822–2835.

Bendahmane A, Farnham G, Moffett P, Baulcombe DC. 2002. Constitutive gain-of-function mutants in a nucleotide binding site-leucine rich repeat protein encoded at the *Rx* locus of potato. *The Plant Journal* 32: 195–204.

Bonardi V, Tang S, Stallmann A, Roberts M, Cherkis K, Dangl JL. 2011. Expanded functions for a family of plant intracellular immune receptors beyond specific recognition of pathogen effectors. *Proceedings of the National Academy of Sciences, USA* 108: 16463–16468.

Broggini GA, Wohner T, Fahrentrapp J, Kost TD, Flachowsky H, Peil A, Hanke MV, Richter K, Patocchi A, Gessler C. 2014. Engineering fire blight resistance into the apple cultivar 'Gala' using the *FB_MR5* CC-NBS-LRR resistance gene of *Malus x robusta* 5. *Plant Biotechnology Journal* 12: 728–733.

Carter ME, Helm M, Chapman A, Wan E, Restrepo Sierra AM, Innes R, Bogdanove AJ, Wise RP. 2018. Convergent evolution of effector protease recognition by *Arabidopsis* and barley. *Molecular Plant–Microbe Interactions* 32: 550–565.

Chen Z, Kloek AP, Cuzick A, Moeder W, Tang D, Innes RW, Klessig DF, McDowell JM, Kunkel BN. 2004. The *Pseudomonas syringae* type III effector AvrRpt2 functions downstream or independently of SA to promote virulence on *Arabidopsis thaliana*. *The Plant Journal* 37: 494–504.

Cherkis KA, Temple BR, Chung EH, Sondek J, Dangl JL. 2012. AvrRpm1 missense mutations weakly activate RPS2-mediated immune response in *Arabidopsis thaliana*. *PLoS ONE* 7: e42633.

Chisholm ST, Dahlbeck D, Krishnamurthy N, Day B, Sjolander K, Staskawicz BJ. 2005. Molecular characterization of proteolytic cleavage sites of the *Pseudomonas syringae* effector AvrRpt2. *Proceedings of the National Academy of Sciences, USA* 102: 2087–2092.

Chung EH, da Cunha L, Wu AJ, Gao Z, Cherkis K, Afzal AJ, Mackey D, Dangl JL. 2011. Specific threonine phosphorylation of a host target by two unrelated type III effectors activates a host innate immune receptor in plants. *Cell Host & Microbe* 9: 125–136.

Chung EH, El-Kasmi F, He Y, Loehr A, Dangl JL. 2014. A plant phosphoswitch platform repeatedly targeted by type III effector proteins regulates the output of both tiers of plant immune receptors. *Cell Host & Microbe* 16: 484–494.

Clough SJ, Bent AF. 1998. Floral dip: a simplified method for *Agrobacterium*-mediated transformation of *Arabidopsis thaliana*. *The Plant Journal* 16: 735–743.

Coaker G, Falick A, Staskawicz B. 2005. Activation of a phytopathogenic bacterial effector protein by a eukaryotic cyclophilin. *Science* 308: 548–550.

Coaker G, Zhu G, Ding Z, Van Doren SR, Staskawicz B. 2006. Eukaryotic cyclophilin as a molecular switch for effector activation. *Molecular Microbiology* 61: 1485–1496.

Cui F, Wu S, Sun W, Coaker G, Kunkel B, He P, Shan L. 2013. The *Pseudomonas syringae* type III effector AvrRpt2 promotes pathogen virulence via stimulating *Arabidopsis* auxin/indole acetic acid protein turnover. *Plant Physiology* 162: 1018–1029.

Day B, Dahlbeck D, Huang J, Chisholm ST, Li D, Staskawicz BJ. 2005. Molecular basis for the RIN4 negative regulation of RPS2 disease resistance. *Plant Cell* 17: 1292–1305.

DeYoung BJ, Qi D, Kim SH, Burke TP, Innes RW. 2012. Activation of a plant nucleotide binding-leucine rich repeat disease resistance protein by a modified self protein. *Cellular Microbiology* 14: 1071–1084.

Dodds PN, Rathjen JP. 2010. Plant immunity: towards an integrated view of plant-pathogen interactions. *Nature Reviews Genetics* 11: 539–548.

El Kasmi F, Chung EH, Anderson RG, Li J, Wan L, Eitas TK, Gao Z, Dangl JL. 2017. Signaling from the plasma-membrane localized plant immune receptor RPM1 requires self-association of the full-length protein. *Proceedings of the National Academy of Sciences, USA* 114: E7385–E7394.

Engler C, Kandzia R, Marillonnet S. 2008. A one pot, one step, precision cloning method with high throughput capability. *PLoS ONE* 3: e3647.

Eschen-Lippold L, Jiang X, Elmore JM, Mackey D, Shan L, Coaker G, Scheel D, Lee J. 2016. Bacterial AvrRpt2-like cysteine proteases block activation of the *Arabidopsis* mitogen-activated protein kinases, MPK4 and MPK11. *Plant Physiology* 171: 2223–2238.

Jayaraman J, Choi S, Prokchorchik M, Choi DS, Spiandore A, Rikkerink EH, Templeton MD, Segonzac C, Sohn KH. 2017. A bacterial acetyltransferase triggers immunity in *Arabidopsis thaliana* independent of hypersensitive response. *Scientific Reports* 7: 3557.

Jeuken MJ, Zhang NW, McHale LK, Pelgrom K, den Boer E, Lindhout P, Michelmore RW, Visser RG, Niks RE. 2009. *Rin4* causes hybrid necrosis and

race-specific resistance in an interspecific lettuce hybrid. *Plant Cell* 21: 3368–3378.

Jin P, Wood MD, Wu Y, Xie Z, Katagiri F. 2003. Cleavage of the *Pseudomonas syringae* type III effector AvrRpt2 requires a host factor(s) common among eukaryotes and is important for AvrRpt2 localization in the host cell. *Plant Physiology* 133: 1072–1082.

Jones JD, Dangl JL. 2006. The plant immune system. *Nature* 444: 323–329.

Kessens R, Ashfield T, Kim SH, Innes RW. 2014. Determining the GmRIN4 requirements of the soybean disease resistance proteins Rpg1b and Rpg1r using a *Nicotiana glutinosa*-based agroinfiltration system. *PLoS ONE* 9: e108159.

Kim HS, Desveaux D, Singer AU, Patel P, Sondek J, Dangl JL. 2005. The *Pseudomonas syringae* effector AvrRpt2 cleaves its C-terminally acylated target, RIN4, from *Arabidopsis* membranes to block RPM1 activation. *Proceedings of the National Academy of Sciences, USA* 102: 6496–6501.

Kim MG, da Cunha L, McFall AJ, Belkhadir Y, DebRoy S, Dangl JL, Mackey D. 2005. Two *Pseudomonas syringae* type III effectors inhibit RIN4-regulated basal defense in *Arabidopsis*. *Cell* 121: 749–759.

Lee J, Manning AJ, Wolfgeher D, Jelenska J, Cavanaugh KA, Xu H, Fernandez SM, Michelmore RW, Kron SJ, Greenberg JT. 2015. Acetylation of an NB-LRR plant immune-effector complex suppresses immunity. *Cell Reports* 13: 1670–1682.

Liu J, Elmore JM, Lin ZJ, Coaker G. 2011. A receptor-like cytoplasmic kinase phosphorylates the host target RIN4, leading to the activation of a plant Innate immune receptor. *Cell Host & Microbe* 9: 137–146.

Luo Y, Caldwell KS, Wroblewski T, Wright ME, Michelmore RW. 2009. Proteolysis of a negative regulator of innate immunity is dependent on resistance genes in tomato and *Nicotiana benthamiana* and induced by multiple bacterial effectors. *Plant Cell* 21: 2458–2472.

Mackey D, Belkhadir Y, Alonso JM, Ecker JR, Dangl JL. 2003. *Arabidopsis* RIN4 is a target of the type III virulence effector AvrRpt2 and modulates RPS2-mediated resistance. *Cell* 112: 379–389.

Mackey D, Holt BF 3rd, Wiig A, Dangl JL. 2002. RIN4 interacts with *Pseudomonas syringae* type III effector molecules and is required for RPM1-mediated resistance in *Arabidopsis*. *Cell* 108: 743–754.

Nimchuk Z, Marois E, Kjemtrup S, Leister RT, Katagiri F, Dangl JL. 2000. Eukaryotic fatty acylation drives plasma membrane targeting and enhances function of several type III effector proteins from *Pseudomonas syringae*. *Cell* 101: 353–363.

Oh CS, Pedley KF, Martin GB. 2010. Tomato 14-3-3 protein 7 positively regulates immunity-associated programmed cell death by enhancing protein abundance and signaling ability of MAPKKKα. *Plant Cell* 22: 260–272.

Rikkerink EHA. 2018. Pathogens and disease play havoc on the host epiproteome-the "first line of response" role for proteomic changes influenced by disorder. *International Journal of Molecular Sciences* 19: E772.

Rodriguez E, El Ghoul H, Mundy J, Petersen M. 2016. Making sense of plant autoimmunity and 'negative regulators'. *The FEBS Journal* 283: 1385–1391.

Schropfer S, Bottcher C, Wohner T, Richter K, Norelli J, Rikkerink EHA, Hanke MV, Flachowsky H. 2018. A single effector protein, AvrRpt2$_{EA}$, from *Erwinia amylovora* can cause fire blight disease symptoms and induces a salicylic acid-dependent defense response. *Molecular Plant–Microbe Interactions* 31: 1179–1191.

Selote D, Kachroo A. 2010. RPG1-B-derived resistance to *AvrB*-expressing *Pseudomonas syringae* requires RIN4-like proteins in soybean. *Plant Physiology* 153: 1199–1211.

Shao F, Golstein C, Ade J, Stoutemyer M, Dixon JE, Innes RW. 2003. Cleavage of *Arabidopsis* PBS1 by a bacterial type III effector. *Science* 301: 1230–1233.

Simonich M, Innes R. 1995. A disease resistance gene in *Arabidopsis* with specificity for the *avrPph3* gene of *Pseudomonas syringae* pv. *phaseolicola*. *Molecular Plant–Microbe Interactions* 8: 637–40.

Sun J, Huang G, Fan F, Wang S, Zhang Y, Han Y, Zou Y, Lu D. 2017. Comparative study of *Arabidopsis* PBS1 and a wheat PBS1 homolog helps understand the mechanism of PBS1 functioning in innate immunity. *Scientific Reports* 7: 5487.

Sun X, Greenwood DR, Templeton MD, Libich DS, McGhie TK, Xue B, Yoon M, Cui W, Kirk CA, Jones WT *et al.* 2014. The intrinsically disordered structural platform of the plant defence hub protein RPM1-interacting protein 4 provides insights into its mode of action in the host-pathogen interface and evolution of the nitrate-induced domain protein family. *The FEBS Journal* 281: 3955–3979.

Swiderski MR, Innes RW. 2001. The *Arabidopsis* PBS1 resistance gene encodes a member of a novel protein kinase subfamily. *The Plant Journal* 26: 101–112.

Takemoto D, Jones DA. 2005. Membrane release and destabilization of *Arabidopsis* RIN4 following cleavage by *Pseudomonas syringae* AvrRpt2. *Molecular Plant–Microbe Interactions* 18: 1258–1268.

Takken FL, Albrecht M, Tameling WI. 2006. Resistance proteins: molecular switches of plant defence. *Current Opinion in Plant Biology* 9: 383–390.

Thomas WJ, Thireault CA, Kimbrel JA, Chang JH. 2009. Recombineering and stable integration of the *Pseudomonas syringae* pv. *syringae* 61 *hrp/hrc* cluster into the genome of the soil bacterium *Pseudomonas fluorescens* Pf0-1. *The Plant Journal* 60: 919–928.

Toruno TY, Shen M, Coaker G, Mackey D. 2018. Regulated disorder: posttranslational modifications control the RIN4 plant immune signaling hub. *Molecular Plant–Microbe Interactions* 32: 56–64.

van der Hoorn RA, Kamoun S. 2008. From guard to decoy: a new model for perception of plant pathogen effectors. *Plant Cell* 20: 2009–2017.

Vogt I, Wohner T, Richter K, Flachowsky H, Sundin GW, Wensing A, Savory EA, Geider K, Day B, Hanke MV *et al.* 2013. Gene-for-gene relationship in the host-pathogen system *Malus x robusta* 5-*Erwinia amylovora*. *New Phytologist* 197: 1262–1275.

Wang Y, Li J, Hou S, Wang X, Li Y, Ren D, Chen S, Tang X, Zhou JM. 2010. A *Pseudomonas syringae* ADP-ribosyltransferase inhibits *Arabidopsis* mitogen-activated protein kinase kinases. *Plant Cell* 22: 2033–2044.

Whalen MC, Innes RW, Bent AF, Staskawicz BJ. 1991. Identification of *Pseudomonas syringae* pathogens of *Arabidopsis* and a bacterial locus determining avirulence on both *Arabidopsis* and soybean. *Plant Cell* 3: 49–59.

Wilton M, Subramaniam R, Elmore J, Felsensteiner C, Coaker G, Desveaux D. 2010. The type III effector HopF2$_{Pto}$ targets *Arabidopsis* RIN4 protein to promote *Pseudomonas syringae* virulence. *Proceedings of the National Academy of Sciences, USA* 107: 2349–2354.

Xu N, Luo X, Li W, Wang Z, Liu J. 2017. The bacterial effector AvrB-induced RIN4 hyperphosphorylation is mediated by a receptor-like cytoplasmic kinase complex in *Arabidopsis*. *Molecular Plant–Microbe Interactions* 30: 502–512.

Yamada T. 1993. The role of auxin in plant-disease development. *Annual Review of Phytopathology* 31: 253–273.

Zhao Y, He SY, Sundin GW. 2006. The *Erwinia amylovora* avrRpt2$_{EA}$ gene contributes to virulence on pear and AvrRpt2$_{EA}$ is recognized by *Arabidopsis* RPS2 when expressed in *Pseudomonas syringae*. *Molecular Plant–Microbe Interactions* 19: 644–654.

Supporting Information

Additional Supporting Information may be found online in the Supporting Information section at the end of the article.

Fig. S1 Phylogenetic analysis of the selected CNLs from multiple plant species.

Fig. S2 MdRIN4-2 and RIN4 homologs from *Pyrus* species can activate MR5 upon AvrRpt2-directed cleavage.

Fig. S3 RIN4 homologs from *N. benthamiana* cannot suppress RPS2 auto-activity or activate MR5 when co-expressed with EaAvrRpt2.

Fig. S4 Phylogenetic tree of RIN4 homologs from diverse plant species.

Fig. S5 F179A substitution of MdRIN4 abolish AvrRpt2-triggered and MR5-dependent induction of ion leakage.

Fig. S6 Reciprocal mutations at D/N or F/Y amino acid residues dramatically alter chimeric RIN4 ACP3 function.

Fig. S7 MdRIN4$^{D186N/F193Y}$ suppresses RPS2 auto-activity when co-expressed with AvrRpt2.

Fig. S8 Full-length RIN4 variants with mutations in polymorphic residues accumulate to higher levels and can be eliminated by AvrRpt2 when expressed *in planta*.

Fig. S9 The palmitoylation sequence motif is required for function of RIN4 full-length and ACP3 variants carrying reciprocal mutations at D/N or F/Y amino acid residues.

Fig. S10 MdRIN4$^{D186N/F193Y}$ ACP3 variant can suppress RPM1 and RPS2 mediated autoimmunity.

Fig. S11 *RIN4* transgene expression in Arabidopsis transgenic lines.

Methods S1 Quantitative RT-PCR.

Methods S2 RIN4 homolog and CNL phylogenetic analysis.

Table S1 Primers used in this study.

Table S2 Table of approximate molecular weights of protein products and their fragments used in this study.

Please note: Wiley Blackwell are not responsible for the content or functionality of any Supporting Information supplied by the authors. Any queries (other than missing material) should be directed to the *New Phytologist* Central Office.